



Diagnostic value of the flare sign in predicting extracapsular extension in metastatic axillary lymph nodes and nodal status on breast magnetic resonance imaging

Cihan Özgür¹
 Baran Serdar Sunal¹
 Savaş Hereklioğlu¹
 Meltem Öznur²
 Sibel Özkan Gürdal³

¹Tekirdağ Namık Kemal University Faculty of Medicine, Department of Radiology, Tekirdağ, Türkiye

²Tekirdağ Namık Kemal University Faculty of Medicine, Department of Pathology, Tekirdağ, Türkiye

³Tekirdağ Namık Kemal University Faculty of Medicine, Department of Surgical Oncology, Tekirdağ, Türkiye

PURPOSE

This study aimed to evaluate the diagnostic performance of breast magnetic resonance imaging (MRI) in predicting extracapsular extension (ECE) and axillary nodal status in the axillary metastatic lymph nodes of patients with breast cancer.

METHODS

The preoperative MRI scans of 92 patients with breast cancer and axillary metastases who did not receive neoadjuvant treatment between January 2018 and January 2024 were retrospectively examined. The presence of an increased signal in the axillary fatty tissue surrounding the lymph node (flare sign) on T2-weighted images, irregular nodal contour (shaggy margin), axillary asymmetry (difference in the number and size of lymph nodes compared with the unaffected axilla), loss of the fatty hilum in the most suspicious lymph node, and morphological features on T1-weighted images were assessed. Each dissected axillary lymph node was examined for ECE, and the histopathological results were recorded.

RESULTS

Axillary flare sign was significantly associated with the presence of ECE ($P < 0.001$), number of lymph nodes with ECE ($P < 0.001$), the presence of ≥ 4 axillary metastatic lymph nodes ($P < 0.001$), size of the primary tumor ($P = 0.033$), lymphovascular invasion in the primary tumor ($P < 0.001$), and presence of perineural invasion ($P = 0.001$). The flare sign exhibited 65.7% sensitivity, 96% specificity, 97.8% positive predictive value, 51.1% negative predictive value, and 73.9% accuracy in predicting ECE. Additionally, the receiver operating characteristic curve analysis revealed an area under the curve of 0.808 (95% confidence interval: 0.719–0.898).

CONCLUSION

The flare sign has high performance in predicting ECE and axillary nodal status and is associated with primary tumor aggressiveness, indicating its potential utility in preoperative evaluation.

CLINICAL SIGNIFICANCE

The flare sign on breast MRI may play a crucial role in preoperative planning, surgical decision-making, and axillary status assessment by accurately predicting ECE.

KEYWORDS

Axilla, breast neoplasms, extranodal extension, lymphadenopathy, lymph node, magnetic resonance imaging

Corresponding author: Cihan Özgür

E-mail: cihanozguritf@gmail.com

Received 25 June 2024; revision requested 30 July 2024; accepted 10 October 2024.



Epub: 07.11.2024

Publication date: xx.xx.2024

DOI: 10.4274/dir.2024.242906

The clinical evaluation of patients with breast cancer involves determining the presence of axillary node metastases as a prognostic indicator, in addition to tumor size.¹ Assessing the axilla using radiology is essential for managing breast cancer, as it provides crucial insights into locoregional staging for surgical procedures. The Breast Imaging Reporting and

Data System lexicon for preoperative breast magnetic resonance imaging (MRI) assessment evaluates axillary lymph nodes within the field of view as “associated features,” even though ultrasound remains essential for determining axillary status.² Extracapsular extension (ECE) occurs when malignant cells invade the surrounding tissue by breaching the capsule of a lymph node.³ There is still a lack of understanding regarding the specific biological mechanisms responsible for ECE. Increased vessel permeability, inflammation around the lymph nodes, and the obstruction of lymphatic channels may indicate that the tumor is aggressive in lymph nodes and lymphatic vessels.⁴ Unlike the previous tumor–node–metastasis classification, the current classification excludes the evaluation of ECE. The most recent reporting protocol from the College of American Pathologists recommends documenting the presence of ECE in metastatic axillary lymph nodes.⁵ Yang et al.⁶ linked the presence of ECE in sentinel lymph nodes (SLNs) to advanced tumor stage, progesterone receptor (PR) status, lymphovascular invasion, increased metastasis rates in non-SLNs, nodal burden, the number of affected non-SLNs, and the total number of positive lymph nodes. Patients with ECE exhibit a significantly higher incidence of pN2 disease. In SLNs, ECE significantly decreases disease-free and overall survival.⁶ Furthermore, ECE in metastatic SLNs is a strong indicator of residual axillary disease.^{7,8} Based on these results, it may be more beneficial to forgo SLN biopsy and opt for axillary lymph node dissection (ALND) if ECE is detected.

An irregular shape, unclear margins, and infiltration into nearby tissues observed on

sonography are indicative of ECE. Only a few studies have reported MRI findings, defined as increased T2 signal intensity surrounding the lymph nodes.^{4,9} Researchers have also used these findings to predict lymph node malignancy.¹⁰ Baltzer et al.¹⁰ proposed the term ‘perifocal edema’ to describe this finding, and researchers have reported that it has a sensitivity of 29.4% and a specificity of 100% in accurately discriminating between malignant and benign lymph nodes.

Given the challenges of directly detecting metastatic spread beyond the lymph node capsule with current imaging techniques, this study aimed to determine the utility of breast MRI in correlating changes in fat signals around the axillary lymph nodes with ECE.

Methods

Patients

This retrospective study was approved by the Non-Interventional Clinical Research Ethics Committee of Tekirdağ Namık Kemal University (protocol number: 2024.36.02.20, date: 27.02.2024). The requirement for informed consent was waived because of the retrospective nature of the study. The study initially included 352 patients with pathologically confirmed axillary metastases from breast cancer who underwent axillary dissection (SLN biopsy and/or ALND) between January 2018 and January 2024. Patients without a preoperative MRI examination (n = 52), those with low image resolution or artifacts (n = 30), and those receiving neoadjuvant chemotherapy (NAC) or hormone therapy (n = 178) were excluded. A total of 92 women who underwent breast MRI within 3 months preoperatively were included in the study (Figure 1).

The evaluation of cases also considered age; postoperative tumor and node stages; maximum tumor size; tumor histology; hormone status; Ki67 index; human epidermal growth factor receptor 2 (HER2) positivity; lymphovascular invasion in the primary tumor; the presence of perineural invasion; the number of total, metastatic, and non-metastatic lymph nodes detected in the axilla; and the number of metastatic lymph nodes with ECE.

Histopathological assessment

A pathologist with 16 years of experience in breast pathology conducted the histopathological evaluation of the surgical specimens. The tumor, histological, and molecular subtypes were determined. Hormone (estrogen and progesterone) receptor status, HER2 status, histology (modified Richardson–Bloom score), and nuclear grade were recorded. Patients with estrogen receptor and PR levels >1% were considered positive for hormone receptors. In cases where the HER2 receptor level was +2 (equivocal), the receptor level was verified using fluorescence *in situ* hybridization analysis. Cases in which both receptors were detected as level 0 and +1 were considered negative, and cases in which level +3 was detected were considered positive. The tumor and node stages were evaluated according to the 8th edition of the American Joint Committee on Cancer staging manual.¹¹

In addition, SLNs were identified using 1% isosulfan blue dye solution on biopsies of dye-retaining nodes. During surgery, imprint cytology and the sequential sectioning of SLNs were performed. Tissue blocks were examined for metastatic cells, and positive cases underwent additional ALND. The final diagnosis was determined using paraffin-em-

Main points

- The flare sign is characterized by increased signal intensity surrounding the lymph nodes observed on fat-suppressed T2-weighted images.
- Breast magnetic resonance imaging, particularly when assessing the presence of the flare sign, demonstrated a sensitivity of 65.7%, specificity of 96%, positive predictive value of 97.8%, negative predictive value of 51.1%, and accuracy of 73.9% in detecting extracapsular extension during preoperative evaluation.
- The presence of the axillary flare sign was associated with several factors indicating the aggressiveness of the primary tumor, including the presence of ≥4 axillary metastatic lymph nodes ($P < 0.001$), larger primary tumor size ($P = 0.033$), lymphovascular invasion in the primary tumor ($P < 0.001$), and perineural invasion ($P = 0.001$).

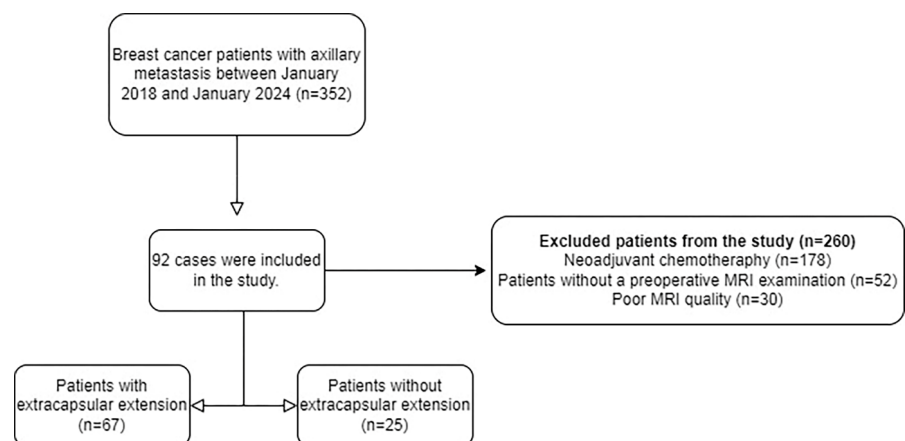


Figure 1. Study participant flow diagram. MRI, magnetic resonance imaging.

bedded tissues stained with hematoxylin and eosin, and metastasis was classified as isolated tumor cells, micrometastasis, and macrometastasis.⁶ Patients with macrometastases in paraffin sections but negative imprint cytology underwent further ALND. Histopathology helped estimate the number of excised benign and metastatic lymph nodes. ECE was defined as positive if a metastatic tumor had spread to the extranodal fat, with or without a desmoplastic stromal response (Figure 2).⁶ The number of metastatic lymph nodes on ECE was also recorded. The length of the ECE, presence of extranodal blood vessel tumor emboli, and extranodal tumor deposits in the metastatic lymph nodes were not evaluated.

Magnetic resonance examination and image acquisition

MRI examinations were performed in the prone position using a 1.5T MRI device (Ingenia; Philips Healthcare, Amsterdam, Netherlands) with a seven-channel dedicated breast coil. The MRI protocol was as follows: axial T2-weighted fat-suppressed sequence [repetition time (TR): 4,317 ms, echo time (TE): 70 ms, slice thickness 3.5 mm, matrix 300 × 258] and T1-weighted turbo spin echo sequence (TR: 490 ms; TE: 8 ms; slice thickness 3.5 mm, matrix 300 × 364); for contrast-enhanced MRI, the gadobutrol dose was 0.1 mmol/kg, and images were obtained six times after saline was injected at a rate of 20 mL/s and then at 2 mL/s. The first imaging was performed 60 s after the contrast injection. Post-contrast sagittal reformatted images were obtained. Images were evaluated using a Picture Archiving Communication System (ISD7, Sectra, Linköping, Sweden). The presence of an increased signal in the axillary fatty tissue surrounding the lymph node (flare sign) on the T2-weighted images, irregular nodal contour (shaggy margin), axillary asymmetry (diagnosed when lymph nodes in the affected axilla differed in number or size compared with the opposite side), loss of the fatty hilum in the most suspicious lymph node, and morphological features (long- and short-axis diameters) were examined on T1-weighted images (Figure 3). Two radiologists with 7- and 6-years' experience in breast radiology retrospectively evaluated the results. The radiologists were blinded to patients' ECE status. Images were reassessed, and a consensus was obtained if the results varied. In case of discrepancies, the two radiologists reached a final decision through discussion.

Statistical analysis

Descriptive analysis was used to determine the frequency and distribution of patient age; postoperative tumor and node stages; maximum tumor size; tumor histology; hormone status; Ki67 index; Cerb2 positivity; lymphovascular invasion in the primary tumor; presence of perineural invasion; number of total, metastatic, and non-metastatic lymph nodes detected in the axilla; and number of metastatic lymph nodes with ECE.

Data analysis was performed using the Statistical Package for Social Sciences (v.25.0, IBM, Armonk, NY, USA). The suitability of continuous variables for a normal distribution was examined using the Shapiro–Wilk test. Receiver operating characteristic (ROC)

curve analysis was performed for parameters that had a significant effect on ECE, and results are presented as area under the curve (AUC), sensitivity and specificity, and 95% confidence intervals (CIs). Sensitivity and specificity were calculated using the Youden index. A logistic regression analysis was performed to determine the effects of various parameters on ECE. Pearson's chi-square test, Fisher's exact test, the Fisher–Freeman–Halton exact test, and Yates correction were used to analyze independent categorical variables. The Mann–Whitney U test was used in two independent group analyses because the data did not exhibit a normal distribution. The statistical significance level was accepted at 0.05.

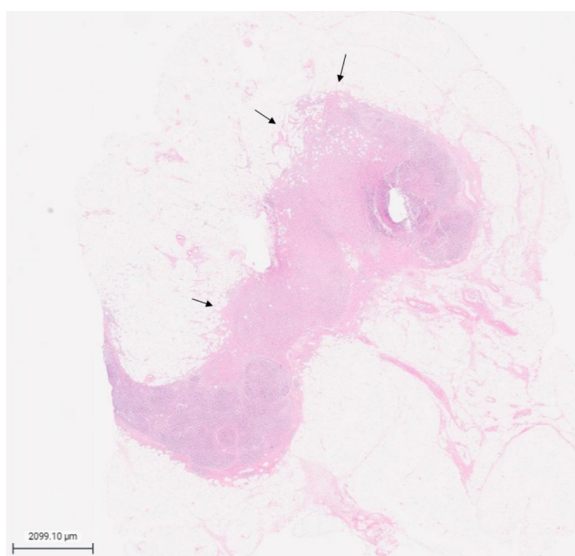


Figure 2. Photomicrograph of a lymph node revealing metastatic cells spreading into extranodal fat (arrows).

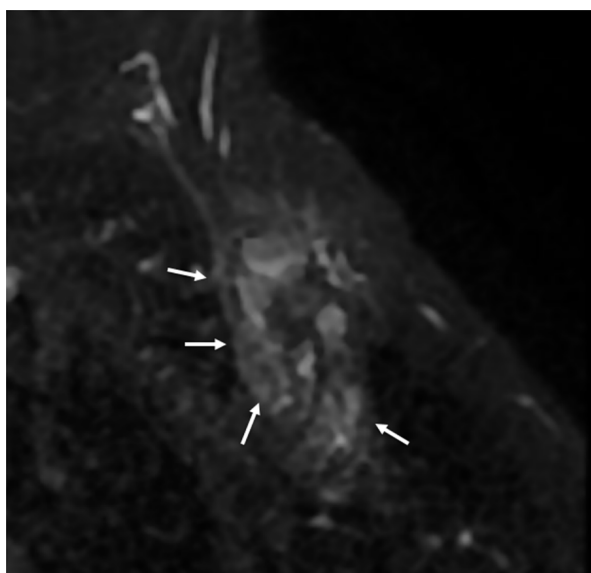


Figure 3. Axial fat-suppressed T2-weighted magnetic resonance image of the axilla in a 65-year-old female patient with invasive ductal carcinoma revealing an increased signal around the metastatic lymph nodes (flare sign) (arrows). Extracapsular extension was detected in five out of eight metastatic lymph nodes as a result of axillary lymph node dissection.

Results

Patient, clinical, and histopathological data

The average age of the 92 women was 55.9 (range: 32–75) years. The most common histological subtype was invasive ductal carcinoma (68.5%). Of the 92 patients, 67 exhibited ECE, whereas the remaining 25 did not exhibit any signs of ECE. The clinical and histopathological data are presented in Table 1.

The mean interval between MRI and surgery was 48 days, with a range of 4–92 days (± 25.5 days). Overall, 35 patients (38%) underwent SLN biopsy, 24 (26.1%) underwent both SLN biopsy and ALND, and 33 (35.9%) underwent ALND. The median number of harvested SLNs was 9 (range: 3–25). Table 2 summarizes the axillary lymph node data.

Statistical analysis

The flare sign, shaggy margin, and presence of at least one of these (flare sign or shaggy margin) were identified as distinguishing variables for ECE in the ROC analysis. The flare sign had an AUC of 0.808 (95% CI: 0.719–0.898; $P < 0.001$); shaggy margin, 0.731 (95% CI: 0.623–0.840; $P < 0.001$); and presence of at least one of these findings, 0.823 (95% CI: 0.723–0.923; $P < 0.001$). The sensitivity of the flare sign was 65.7%, with a specificity of 96.0%, whereas the sensitivity of the shaggy margin was 58.2%, with a specificity of 88.0%. We calculated the sensitivity and specificity for the presence of at least one of the findings (flare sign or shaggy margin) to be 80.6% and 84.0%, respectively (Table 3).

Logistic regression analysis revealed that the existence of a flare sign was associated with an odds ratio (OR) of 45.913 for ECE, whereas a shaggy margin was associated with an OR of 10.214 ($P < 0.001$). The OR was 21.808 when there was either a flare sign or a shaggy margin ($P < 0.001$). The presence of flare signs and/or shaggy margins in cases with ECE was much more frequent than in cases without ECE (Supplementary Table 1).

Patients with flare signs had a greater number of lymph nodes with ECE ($P < 0.001$) and a larger maximal tumor diameter ($P = 0.004$) than those without flare signs. Patients exhibiting flare signs had increased rates of lymphovascular invasion, perineural invasion, and the presence of ≥ 4 metastatic lymph nodes in the axilla. The presence of a flare sign was not associated with the Ki67 index or histological grade (Table 4).

Discussion

Multiple studies have examined the edema surrounding breast masses, while research on the axilla remains limited. This finding is associated with malignancy¹² and is a key indicator of breast cancer aggressiveness, recurrence, and prognosis.^{13,14}

Prediction of the presence of ECE has been frequently studied in head and neck malignancies in the radiology literature. Kimura et al.¹⁵ defined the characteristics that they investigated for the existence of

ECE as flare sign and shaggy margin. Researchers determined that the flare sign has the following diagnostic performance metrics for detecting ECE: sensitivity, 77%; specificity, 93%; accuracy, 88%; positive predictive value, 83%; and negative predictive value, 90%. We determined that some diagnostic metrics, specifically the positive predictive value, sensitivity, and specificity, were similar in our study, despite focusing on completely different anatomical locations.

The literature contains only a limited number of publications aimed at detecting ECE

Table 1. Clinical and histopathological features of the patients

	Patients (n = 92)
Median age (years) (range)	55.9 (32–75)
Median tumor size (mm) (range)	28.6 (7–160)
Receptor status	
HR+/HER2-	77 (83.7%)
HR+/HER2+	7 (7.6%)
HR-/HER2+	3 (3.3%)
HR-/HER2-	5 (5.4%)
Histologic subtype	
Ductal	63 (68.5%)
Lobular/mixed	15 (16.3%)
Other	14 (15.2%)
Lymphovascular invasion	
Absent	39 (42.4%)
Present	53 (57.6%)
Perineural invasion	
Absent	34 (37%)
Present	58 (63%)
Necrosis	
Absent	79 (85.9%)
Present	13 (14.1%)
Calcification	
Absent	62 (67.4%)
Present	30 (32.6%)
Ki67 (%)	
<14	7 (7.6%)
≥ 14	85 (92.4%)
Clinical T stage	
T1 (≤ 2 cm)	40 (43.5%)
T2 (>2–5 cm)	42 (45.7%)
T3 (>5 cm)	8 (8.7%)
T4	2 (2.2%)
Tumor grade (Scarff–Bloom–Richardson)	
1	4 (4.3%)
2	57 (62%)
3	20 (21.7%)

HER2, human epidermal growth factor receptor 2; HR, hormone receptor.

using breast MRI. In a review by Gupta et al.¹⁶, perinodal edema was identified as a specific ECE indicator. It manifests as a hyperechoic halo surrounding the lymph nodes on ultrasound, blurring of the lymph node margins on computed tomography, and areas of T2 hyperintensity in the perinodal fat on MRI.¹⁶ However, these findings are not supported by specific studies. In the study by Kim et al.⁴, ECE was defined as “the presence of strand-like or circumferential T2 high-signal intensities surrounding the nodes.” A similar methodology was used in the present study. The study reported strong agreement in the assessment of perinodal infiltration (k: 0.74; 95% CI: 0.64–0.85), emphasizing that cases with perinodal infiltration were associated with sentinel node identification. However, that study did not conduct a histopathological examination of the axillary lymph nodes in the presence of ECE, and it included patients with a history of NAC. The perinodal infiltration area also has the potential to respond to NAC. By contrast, our study did not include patients who received NAC, and we assessed the presence of ECE individually in each dissected lymph node. The study by Loissele et al.¹⁷, which involved small patient groups, reported the sensitivity of the peak enhancement level on MRI for detecting ECE as 60% and specificity as 100%. However, this study included only five patients with ECE. Misselt et al.¹⁸ discovered on ultrasonography that unclear margins, node matting, and perinodal edema had high specificity (87%, 84%, and 75%, respectively) but low sensitivity (34%, 52%, and 64%, respectively) in detecting ECE. In our study, we considered the presence of perinodal edema to be equivalent to a flare sign. Notably, MRI has comparable sensitivity but greater specificity. When the presence of a shaggy margin was evaluated alongside a flare sign, sensitivity increased considerably, although this was accompanied by a decrease in specificity.

Our findings suggest that the flare sign is useful in nodal staging, as we found a significant association between its presence and N2 or higher axillary involvement. These results are consistent with those of other studies that have reported the utility of breast MRI in predicting advanced axillary involvement.^{19–21} The American College of Surgeons Oncology Group Z0011 study revealed that ALND may not be necessary in early-stage breast cancer with metastases detected in one or two SLNs.²² However, the study did not establish specific exclusion criteria for patients with ECE. Our findings indicate that ECE may influence axillary management. The

high number of metastatic axillary lymph nodes observed in patients with ECE may support the consideration of ALND without

prior SLN biopsy. Supporting this, a study involving 655 patients demonstrated that ECE detected in SLNs was associated with

Table 2. Features of axillary lymph nodes

	All patients (n = 92)	Patients with ECE (n = 67)	Patients without ECE (n = 25)
Axillary surgery			
Sentinel lymph node biopsy	35	17	18
Axillary lymph node dissection	33	27	6
Conversion to axillary lymph node dissection	24	23	1
Number of lymph nodes removed (median, range)	9 (3–25)	10 (3–25)	5 (3–20)
Number of positive lymph nodes removed			
0	0	0	0
1–3	56	32	24
≥4	36	35	1
N stage			
N0i+	1	0	1
N1mi	3	0	3
N1 (1–3)	54	34	20
N2 (4–9)	24	24	0
N3 (≥10)	10	9	1
Number of examined lymph nodes (mean)	9.6	10.5	6.9
Number of metastatic lymph nodes (mean, range)	4.1 (1–22)	5 (1–22)	1.6 (1–11)
ECE in metastatic lymph nodes			
Number of patients	67	67	0
Number of lymph nodes (mean, range)	3.13 (1–12)		0
Asymmetry	55/92 (63%)	46	9
Loss of fatty hilum	20/92 (21.7%)	16	4
Long-axis diameter (mm) (range)	18.3 (6–44)	18.7 (6–44)	17.3 (8–35)
Short-axis diameter (mm) (range)	9.9 (4–23)	10.4 (4–23)	8.4 (5–22)
Long/short axis ratio	1.9 (1.1–3.8)	1.8 (1.1–3.3)	2.1 (1.3–3.4)
Cortical thickness (mm) (range)	4.4 (1.9–11) (72/92)	4.7 (2.1–11) (51/67)	3.6 (1.9–6.3) (21/25)
Cortical thickness type			
Homogeneous	26/92 (28.2%)	17	9
Non-homogeneous	58/92 (63%)	44	14
Nodular	8/92 (8.7%)	6	2
Flare sign	45/92 (48.9%)	44/67 (65.7%)	1/25 (4%)
Shaggy margin	42/92 (45.7%)	39/67 (58.2%)	3/25 (12%)

ECE, extracapsular extension.

Table 3. Receiver operating characteristic analysis results for parameters that have a significant effect on extracapsular extension

Variables	AUC (95% CI)	P*	Sensitivity (%)	Specificity (%)	PPV	NPV	Accuracy
Flare sign	0.808 (0.719–0.898)	<0.001	65.7	96	97.8	51.1	73.9
Shaggy margin	0.731 (0.623–0.840)	0.001	58.2	88	92.9	44	66.3
Flare sign and/or shaggy margin	0.823 (0.723–0.923)	<0.001	80.6	84	93.1	61.8	81.5

*Receiver operating characteristic analysis, AUC, area under the receiver operating characteristic curve; CI, confidence interval; PPV, positive predictive value; NPV, negative predictive value.

Table 4. Relationship of the flare sign to various parameters

Variables	β	P^*	OR	95% CI	
Number of metastatic lymph nodes with ECE	1.019	<0.001	2.771	1.746	4.399
Tumor size	0.037	0.033	1.038	1.003	1.074
Lymphovascular invasion	1.954	<0.001	7.059	2.752	18.108
Perineural invasion	1.514	0.001	4.545	1.796	11.501
Four or more metastatic lymph nodes	2.338	<0.001	10.357	3.777	28.398
Tumor ki67 index	1.034	0.232	2.812	0.517	15.307
Grade	0.057	0.897	1.059	0.448	2.5

*Logistic regression analysis; OR, odds ratio; CI, confidence interval; ECE, extracapsular extension.

increased axillary nodal burden, disease recurrence, and overall mortality.²³ Additionally, we noted a significantly higher number of non-SLN-positive metastatic axillary lymph nodes in these cases. Another study involving 221 patients indicated that the presence of ECE was directly proportional to the number of involved axillary lymph nodes and disease stage,²⁴ highlighting its potential implications in clinical decision-making.

Our study demonstrated that the flare sign was significantly associated with perineural and lymphovascular invasion in the primary tumor. Reports suggest that perineural and lymphovascular invasion play a significant role in predicting survival outcomes.^{25,26} Therefore, the flare sign, which indicates tumor aggressiveness, has the potential to serve as a prognostic biomarker.

This study has some limitations. Owing to the prolonged interval between MRI and surgery, the findings may change, potentially affecting the results of the study. Furthermore, the length of ECE was not assessed in our study. The length of the ECE may be valuable in certain cases in which false negativity is reported. In their study of 11,730 patients, Gooch et al.²⁷ identified ECE in 2.8% of cases. The study revealed a higher rate of detection of ≥ 4 metastatic lymph nodes in cases with ECE measuring >2 mm than in cases with ECE measuring <2 mm. Extranodal tumor blood vessel embolisms (ENBTVE) and deposits can occur concurrently or independently in the axilla, but ENBTVE was not assessed during pathological examinations conducted in our study. Some cases in which the axillary flare sign is observed may be attributed to these factors. Further studies are required to address this issue. We performed only SLN surgery in some cases. The literature reports a false negative rate of 8.3% for SLN biopsy, and pathological sampling may not have included all cases with possible ECE.²⁸ Similarly, the pathology specimens did not reveal any extranodal tumor deposits. The increased

signal intensity in the axillary fatty tissue may also be caused by isolated tumor deposits. We excluded certain cases from the evaluation due to MRI artifacts and inadequate axillary inclusion in the field of view. This may have also affected our results.

In conclusion, this study demonstrates that the flare sign on breast MRI is a highly valuable diagnostic marker for predicting ECE and axillary nodal status in patients with breast cancer. It exhibits high specificity and positive predictive value. Furthermore, its association with tumor aggressiveness, including lymphovascular and perineural invasion, highlights its prognostic value. Incorporating flare sign into preoperative assessment shows promise in determining the status of metastatic axillary lymph nodes. Further studies with larger patient cohorts are warranted to validate these findings.

Conflict of interest disclosure

The authors declared no conflicts of interest.

References

- Kuerer HM. Kuerer's Breast Surgical Oncology. New York, NY: The McGraw-Hill Companies; 2010. [\[CrossRef\]](#)
- Morris E, Comstock C, Lee C, Lehman C, Ikeda D, Newstead G. ACR BI-RADS® magnetic resonance imaging. In: ACR BI-RADS® Atlas, Breast Imaging Reporting and Data System. Reston, VA, American College of Radiology. 2013. [\[CrossRef\]](#)
- Tang P, Moravek M, Oprea-Illies G, Mon KS, Pambuccian SE. Extranodal extension, an international survey on its evaluation and reporting in breast cancer patients. *Pathol Res Pract.* 2022;237:154070. [\[CrossRef\]](#)
- Kim WH, Kim HJ, Park CS, et al. Axillary Nodal Burden Assessed with Pretreatment Breast MRI is associated with failed sentinel lymph node identification after neoadjuvant chemotherapy for breast cancer. *Radiology.* 2020;295(2):275-282. [\[CrossRef\]](#)

- Fitzgibbons PL, Connolly JL, Bose S, et al. Protocol for the examination of resection specimens from patients with invasive carcinoma of the breast. Northfield, IL: College of American Pathologists; Version: InvasiveBreast 4.4.0.0. Protocol Posting Date: February 2020 [Accessed June 20, 2024]. [\[CrossRef\]](#)
- Yang X, Ma X, Yang W, Shui R. Clinical significance of extranodal extension in sentinel lymph node positive breast cancer. *Sci Rep.* 2020;10(1):14684. [\[CrossRef\]](#)
- Fujii T, Yanagita Y, Fujisawa T, Hirakata T, Iijima M, Kuwano H. Implication of extracapsular invasion of sentinel lymph nodes in breast cancer: prediction of nonsentinel lymph node metastasis. *World J Surg.* 2010;34(3):544-548. [\[CrossRef\]](#)
- Schwentner L, Dayan D, Wockel A, et al. Is extracapsular nodal extension in sentinel nodes a predictor for nonsentinel metastasis and is there an impact on survival parameters? A retrospective single center cohort study with 324 patients. *Breast J.* 2018;24(4):480-486. [\[CrossRef\]](#)
- Chang JM, Leung JWT, Moy L, Ha SM, Moon WK. Axillary nodal evaluation in breast cancer: state of the art. *Radiology.* 2020;295(3):500-515. [\[CrossRef\]](#)
- Baltzer PA, Dietzel M, Burmeister HP, et al. Application of MR mammography beyond local staging: is there a potential to accurately assess axillary lymph nodes? evaluation of an extended protocol in an initial prospective study. *AJR Am J Roentgenol.* 2011;196(5):W641-647. [\[CrossRef\]](#)
- Amin MB, Greene FL, Edge SB, et al. The Eighth Edition AJCC Cancer Staging Manual: Continuing to build a bridge from a population-based to a more "personalized" approach to cancer staging. *CA Cancer J Clin.* 2017;67(2):93-99. [\[CrossRef\]](#)
- Baltzer PA, Yang F, Dietzel M, et al. Sensitivity and specificity of unilateral edema on T2w-TSE sequences in MR-mammography considering 974 histologically verified lesions. *Breast J.* 2010;16(3):233-239. [\[CrossRef\]](#)
- Chen Y, Wang L, Luo R, Liu H, Zhang Y, Wang D. Focal breast edema and breast edema score on T2-weighted images provides valuable biological information for invasive breast cancer. *Insights Imaging.* 2023;14(1):73. [\[CrossRef\]](#)
- Cheon H, Kim HJ, Kim TH, et al. Invasive breast cancer: prognostic value of peritumoral edema identified at preoperative mr imaging. *Radiology.* 2018;287(1):68-75. [\[CrossRef\]](#)
- Kimura Y, Sumi M, Sakihama N, Tanaka F, Takahashi H, Nakamura T. MR imaging criteria for the prediction of extranodal spread of metastatic cancer in the neck. *AJNR Am J Neuroradiol.* 2008;29(7):1355-1359. [\[CrossRef\]](#)

16. Gupta A, Metcalf C, Taylor D. Review of axillary lesions, emphasising some distinctive imaging and pathology findings. *J Med Imaging Radiat Oncol.* 2017;61(5):571-581. [\[CrossRef\]](#)
17. Loisselle CR, Eby PR, Peacock S, Kim JN, Lehman CD. Dynamic contrast-enhanced magnetic resonance imaging and invasive breast cancer: primary lesion kinetics correlated with axillary lymph node extracapsular extension. *J Magn Reson Imaging.* 2011;33(1):96-101. [\[CrossRef\]](#)
18. Misselt PN, Glazebrook KN, Reynolds C, Degnim AC, Morton MJ. Predictive value of sonographic features of extranodal extension in axillary lymph nodes. *J Ultrasound Med.* 2010;29(12):1705-1709. [\[CrossRef\]](#)
19. Bode M, Schrading S, Masoumi A, et al. Abbreviated MRI for comprehensive regional lymph node staging during pre-operative breast MRI. *Cancers (Basel).* 2023;15(6):1859. [\[CrossRef\]](#)
20. Hyun SJ, Kim EK, Moon HJ, Yoon JH, Kim MJ. Preoperative axillary lymph node evaluation in breast cancer patients by breast magnetic resonance imaging (MRI): can breast MRI exclude advanced nodal disease? *Eur Radiol.* 2016;26(11):3865-3873. [\[CrossRef\]](#)
21. Kuijs VJ, Moosdorff M, Schipper RJ, et al. The role of MRI in axillary lymph node imaging in breast cancer patients: a systematic review. *Insights Imaging.* 2015;6(2):203-215. [\[CrossRef\]](#)
22. Giuliano AE, McCall L, Beitsch P, et al. Locoregional recurrence after sentinel lymph node dissection with or without axillary dissection in patients with sentinel lymph node metastases: the American College of Surgeons Oncology Group Z0011 randomized trial. *Ann Surg.* 2010;252(3):426-432. [\[CrossRef\]](#)
23. Choi AH, Surrusco M, Rodriguez S, et al. Extranodal extension on sentinel lymph node dissection: why should we treat it differently? *Am Surg.* 2014;80(10):932-935. [\[CrossRef\]](#)
24. Ilknur GB, Hilmi A, Tülay C, et al. The importance of extracapsular extension of axillary lymph node metastases in breast cancer. *Tumori.* 2004;90(1):107-111. [\[CrossRef\]](#)
25. Narayan P, Flynn J, Zhang Z, et al. Perineural invasion as a risk factor for locoregional recurrence of invasive breast cancer. *Sci Rep.* 2021;11(1):12781. [\[CrossRef\]](#)
26. Schoppmann SF, Bayer G, Aumayr K, et al. Prognostic value of lymphangiogenesis and lymphovascular invasion in invasive breast cancer. *Ann Surg.* 2004;240(2):306-312. [\[CrossRef\]](#)
27. Gooch J, King TA, Eaton A, et al. The extent of extracapsular extension may influence the need for axillary lymph node dissection in patients with T1-T2 breast cancer. *Ann Surg Oncol.* 2014;21(9):2897-2903. [\[CrossRef\]](#)
28. Wong SL, Edwards MJ, Chao C, et al. Sentinel lymph node biopsy for breast cancer: impact of the number of sentinel nodes removed on the false-negative rate. *J Am Coll Surg.* 2001;192(6):684-689. [\[CrossRef\]](#)

Supplementary Table 1. Parameters significantly affecting extracapsular extension

Variables	β	P^{L}	OR	95% CI	
Flare sign	3.827	<0.001	45.913	5.834	361.304
Shaggy margin	2.324	0.001	10.214	2.783	37.491
Flare sign and/or shaggy margin	3.082	<0.001	21.808	6.382	74.519

^LLogistic regression analysis; OR, odds ratio; CI, confidence interval.